6. S. J. Fonash, *J. Appl. Phys.*, **54,** 1966 (1983).
7. K. Sen, *Phys. Status Solidi A*, **71,** 641 (1982).
8. S. Kar, D. Shanker, S. P. Joshi, and J. Bhattacharya, in the "Proceedings of the XIII IEEE Photovoltaics Specialist Conference," 628 (1978).
9. P. Munz, K. Kirschbann, G. Krazler, and E. Bucher, in the "Proceedings of the XIV IEEE Photovoltaic Specialist Conference," 1360 (1980).
10. H. Sigmund, *This Journal*, **129,** 2809 (1982).
11. A. Cimino, M. Lo Jacono, P. Porta, and M. Valigi, Z. *Physik. Chem.* (Frankfurt), **59,** 134 (1968).
12. J. Switzer, *Chem. Eng. News*, **48,** Sept. 12, 1983 .
13. C. M. Gronet, N. S. Lewis, G. Cogan, and J. Gibbons, *Proc. Natl. Acad. Sci. USA*, **80,** 1152 (1983).
14. D. R. Penn, *J. Electron. Spectrosc. Relat. Phenom.*, **9,** 29 (1976).
15. S. J. Fonash, "Solar Cell Devise Physics," p. 109, Academic Press, Inc., New York (1981).
16. W. G. Townsend, in "Photovoltaic and Photoelectrochemical Solar Energy Conversion," F. Cardon, W. P. Gomes, and W. Dekeyser, Editors, Chap. 2, Plenum Press, New York (1981).

Semiconductor Electrodes

LXI. Photoelectrochemistry of n-ZrS_2 in Aqueous Solutions

Navin Chandra, Jonathan K. Leland,* and Allen J. Bard**

Department of Chemistry, University of Texas at Austin, Austin, Texas 78712

ABSTRACT

The photoelectrochemical response of electrodes of single crystals of the layer-type compound n-ZrS_2 prepared by vapor transport in Fe^{3+}/Fe^{2+}, ferrocyanide/ferricyanide, and iodide solutions was investigated. The flatband potential (V_{FB}) of the electrode in 1*M* NaCl and 0.032*M* HCl solutions, estimated from impedance measurements, was −0.40V *vs.* SCE at *p*H 1.5 and shifted towards more negative values by 54 mV/unit *p*H change to *p*H 12. A two-electrode photoelectrochemical cell with a n-ZrS_2 anode and Pt gauze cathode in a 0.10*M* $FeCl_2$, 0.10*M* $FeCl_3$, and 1.0*M* HCl electrolyte gave a short-circuit photocurrent of 15 mA/cm² and an open-circuit photovoltage of 0.4V under xenon lamp illumination (*ca.* 100 mW/cm²).

We describe here the application of n-type ZrS_2 as an electrode in photoelectrochemical (PEC) cells. Tributsch was the first to propose the application of layer-type compounds as semiconductor electrodes for PEC studies (1), and a number of different compounds have been studied, *e.g.*, MoS_2, $MoSe_2$, WS_2, WSe_2, $ReSe_2$, ReS_2, and $MoTe_2$ [(2-14) and references therein]. Unlike these other materials, the valence band for ZrS_2 is comprised of anion p-like orbitals (15-17) and is not predicted to be as stable toward photocorrosion. Many of these materials are readily synthesized as single crystals and have bandgaps that match the solar spectrum. The surfaces of layer compounds can also frequently be prepared in a relatively defect free form by peeling off a top layer. These fresh surfaces often show a very low density of surface states (3, 18-20).

One previous study of n-ZrS_2 single crystal electrodes has appeared (21). In this work Tributsch showed that En-ZrS_2 could give reasonably high anodic photocurrent densities in HCl and NaOH solutions, but photocorroded to produce a layer of sulfur on its surface. In the present study, we report growth of an n-ZrS_2 crystal by vapor transport and the PEC behavior of n-ZrS_2 electrodes in Fe^{3+}/Fe^{2+}, ferrocyanide/ferricyanide, and iodide solutions. The n-ZrS_2 crystal showed low dark anodic currents and capacitance measurements allowed estimation of the flatband potential (V_{FB}) and doping densities. The effect of *p*H on V_{FB} was investigated and estimates of the band energies were made from the V_{FB} values and the bandgap energy (E_g).

Experimental

Single crystals of n-type ZrS_2 were grown by the vapor transport method (22, 23) with iodine as the transport agent using the following procedure (24). 3.5g of ZrS_2 (Alfa Products, 99%) were placed in a thoroughly cleaned and dried fused quartz ampul (20 cm length, 2.5 cm id) and evacuated for 18h to 10^{-4} torr. The ampul was then filled with He and I_2 was quickly added (0.25g). The ampul contents were cooled under liquid nitrogen, evacuated for 30 min, and flame sealed. This was then placed in a three-zone furnace (Lindberg, Watertown, WI). The crystal growth zone of the tube was heated to 1100°C for 48h while maintaining the other end of the tube (containing the ZrS_2) at 750°C. The temperature of the growth zone was slowly decreased to 800°C, while that of the material zone was raised to 1000°C. This temperature gradient was maintained for 36h, after which the furnace was switched off and allowed to cool to room temperature. A large number of single crystals, some of them as large as 1 cm², were obtained. Powder x-ray diffraction (Philips Electronics Incorporated) with CuKα radiation and a Ni filter was carried out on the ZrS_2 to confirm the structure. The powder pattern obtained matched that of the ASTM card file for ZrS_2 (11-679), while showing very sharp lines and indicating that the material was crystalline. Ohmic contact to the crystals was made by rubbing In-Ga alloy on one side. A copper wire was attached with silver paint (Acme Chemicals and Insulation, New Haven, CT) to the In-Ga alloy smeared crystal surface. Silicone sealant (Dow Corning 732 RTV) was used to mount the electrode at the end of a glass tube and to seal off the silver paint covered surface, the back, and the edges of the crystal. The electrode area exposed to the solution was 0.02 cm². Before each experiment, the electrodes were freshly peeled with tape, immersed in 1.0*M* HCl for 30s, and thoroughly washed with water.

All chemicals were reagent grade. Test solutions were prepared with Millipore water and deaerated with nitrogen for 1h before the experiment. A conventional single compartment cell with a flat Pyrex glass window for illumination of the semiconductor electrode was used. A saturated calomel electrode (SCE) with a saturated KCl agar bridge and a large area Pt gauze electrode were used as reference and counterelectrodes, respectively. A 450W Xe lamp (Oriel Corporation, Stamford, CT) served as the light source. The light was passed through a 10 cm thick water bath to filter the IR components before reaching the electrochemical cell. The intensity of the light was measured by a power meter (Coherent, Model 210). The electrodes were illuminated with a white light intensity of 100 mW/cm².

Current-potential (*i-V*) curves were recorded with a PAR Model 173 potentiostat fitted with a PAR Model 176 current follower, a PAR Model 175 programmer, and a Model 2000 X-Y recorder (Houston Instrument, Austin, TX). The scan rate used was 20 mV/s. The ac impedance studies were carried out with the same instruments and procedures as described previously (20) over frequency ranges of 100-2000 Hz. The action spectrum was recorded

* Electrochemical Society Student Member.
** Electrochemical Society Life Member.

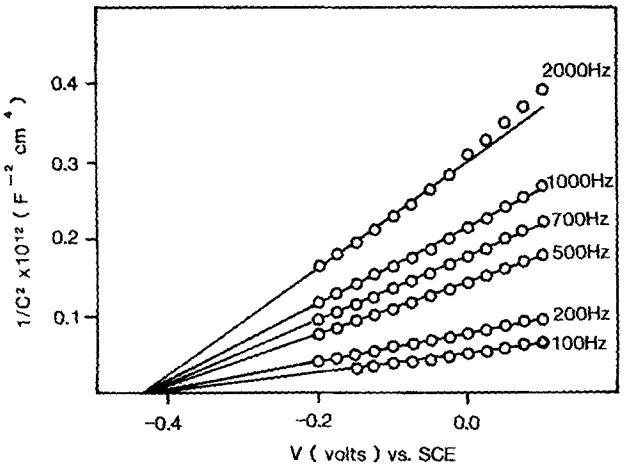

Fig. 1. Mott-Schottky plots for n-ZrS_2 electrode in 1.0M NaCl and 0.032M HCl at pH = 1.5 at the frequencies indicated.

using chopped light (87 Hz) and an Oriel 7240 grating monochromator with a 20 nm bandpass to select the proper wavelength. The electrode potential was held at the equilibrium solution potential (0.24V *vs.* SCE for 0.10*M* $K_3Fe(CN)_6$ and 0.10*M* $K_4Fe(CN)_6$). The modulated photocurrent was detected with a PAR Model 5206 lock-in amplifier, and the photocurrent amplitude and phase angle determined. A plot of photocurrent magnitude *vs.* wavelength yielded the action spectrum after normalizing to the lamp spectrum and correcting for solution absorbance. The radiant light intensity in this experiment was measured with an EG&G (Salem, MA) Model 550 radiometer/photometer. X-ray photoelectron spectroscopy (XPS) measurements were performed with a Vacuum Generators ESCA Lab II system using MgKα radiation.

Results

Effect of pH on V_{FB}.—To study the effect of pH on the V_{FB} for n-ZrS_2, capacitance (C) measurements were carried out in chloride and phosphate buffer solutions. Plots of $1/C^2$ *vs.* *V* [Mott-Schottky (M-S) plots] in 1.0*M* NaCl and 0.032*M* HCl solution at pH 1.5 are shown in Fig. 1. Some frequency dispersion of the capacitance was observed at all pH values. Because the $1/C^2$ *vs.* *V* lines at different frequencies converge at a point on the potential axis, the plots can be used to estimate V_{FB} (25). The V_{FB} *vs.* pH plot (Fig. 2) indicates that the V_{FB} of n-ZrS_2 shifts by *ca.* 54 mV for a unit change in pH. Tributsch (21) also found evidence for a shift in V_{FB} with pH. Although good M-S plots could not be obtained with those samples, the photocurrent curves were shifted along the potential axis for 1*M* HCl compared to 0.5*M* NaOH. This shift, estimated from the difference in potentials for photocurrents at half the saturation value, corresponded to about 27 mV/pH unit. The large shift in V_{FB} with pH found here for ZrS_2, which approaches that found with oxide semiconductors, can be contrasted with the behavior of other layer-type (Group VI metal) compounds. For example, n-MoS_2 shows a shift in photocurrent onset with pH that is more pronounced in strongly alkaline solutions (26). However, M-S plots of n-$MoSe_2$ and p-WSe_2 indicate essentially no change in V_{FB} with pH (3).

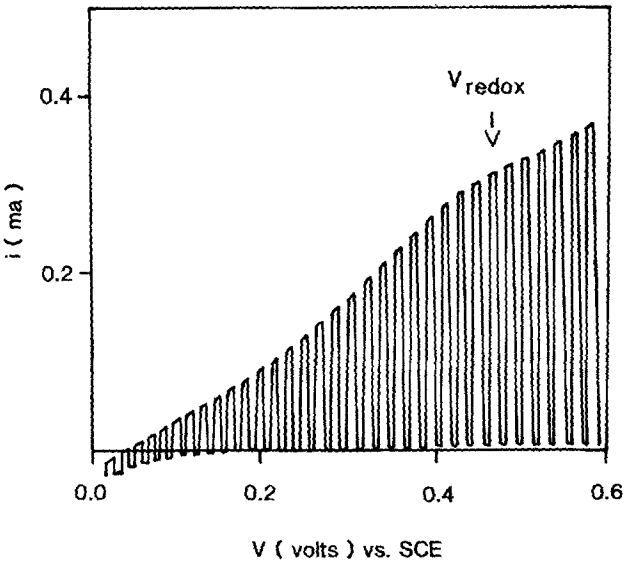

Fig. 3. *i-V* curve for n-ZrS_2 electrode in 0.1M each $FeCl_2$ and $FeCl_3$ in 1.0M HCl under 100 mW/cm², chopped white light illumination. Scan rate: 20 mV/s.

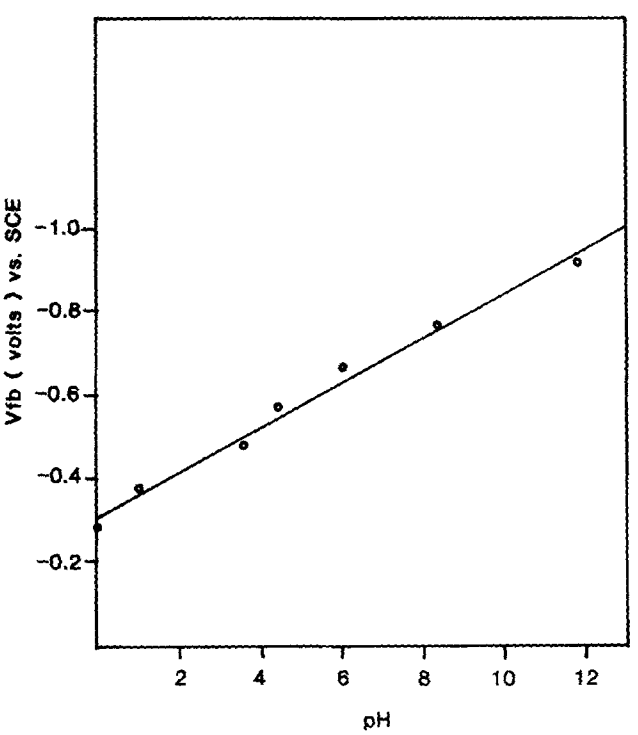

Fig. 2. Flatband potential (V_{FB}) of n-ZrS_2 electrode *vs.* pH

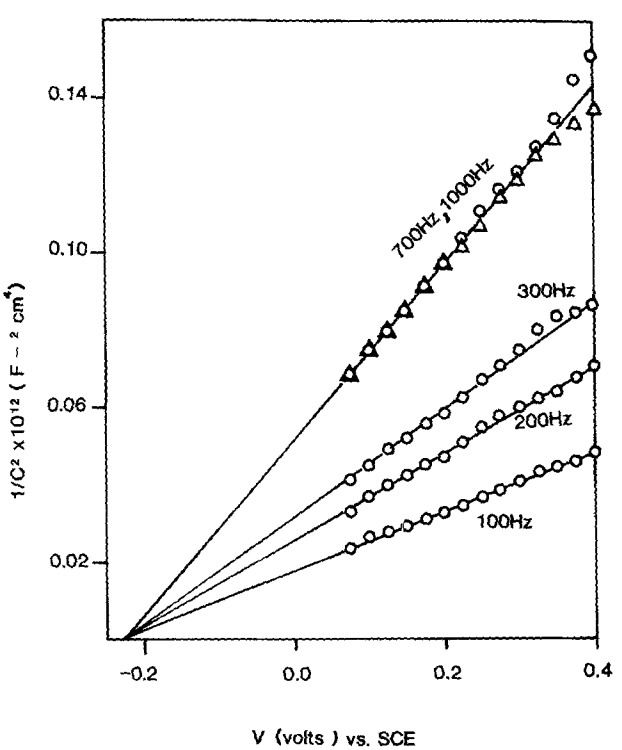

Fig. 4. Mott-Schottky plots for n-ZrS_2 electrode in 0.1M each $FeCl_2$, $FeCl_3$, and 1.0M HCl at the frequencies indicated.

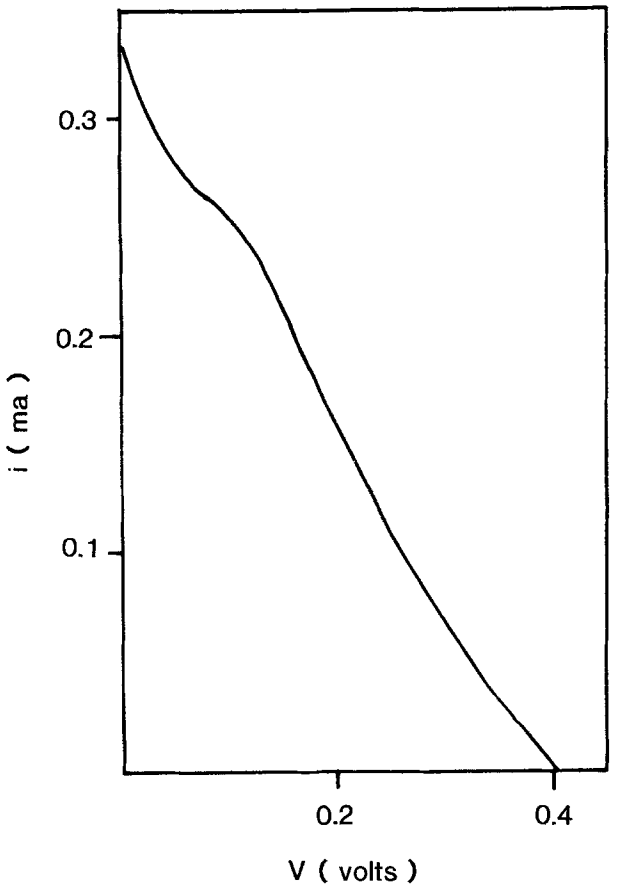

Fig. 5. Power curve for a two-electrode cell with n-ZrS_2 photoanode and a platinum gauze cathode in 0.1M each $FeCl_2$ and $FeCl_3$ in 1.0M HCl under 100 mW/cm², white light illumination.

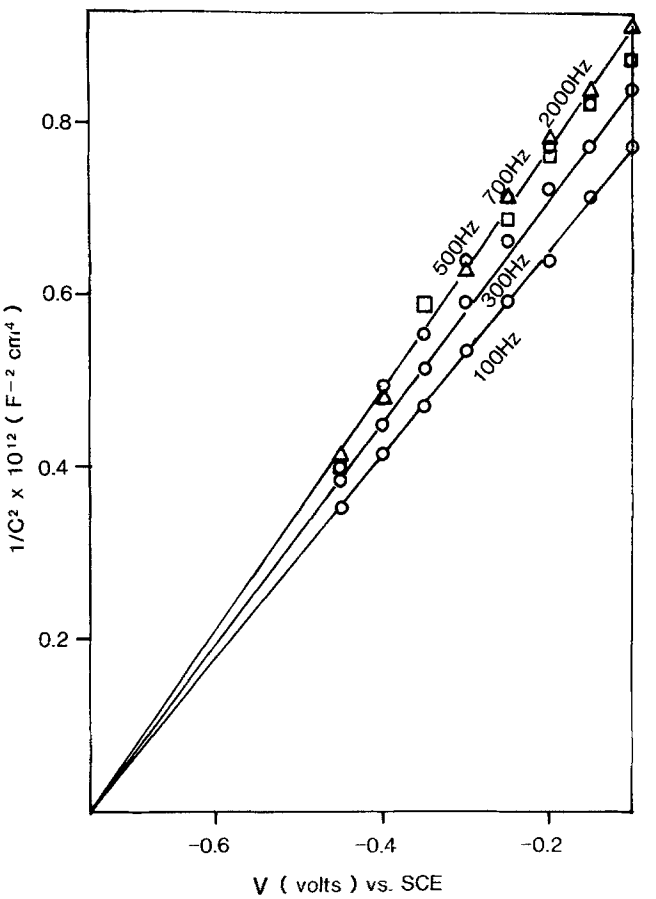

Fig. 6. Mott-Schottky plots for n-ZrS_2 electrode in 0.1M each $K_3Fe(CN)_6$ and $K_4Fe(CN)_6$ (pH = 7.0) at the frequencies indicated.

To investigate the dependency of V_{FB} with pH for n-ZrS_2, XPS measurements were carried out by comparing virgin ZrS_2 crystals to those which were used as electrodes for capacitance measurements. These measurements clearly demonstrate the formation of an oxide layer on electrochemically cycled crystals. The sulfur 2p peak (162.0 eV) was greatly diminished and the Zr $3d_{5/2}$ and $3d_{3/2}$ peaks (181.5 and 184.0 eV, respectively, for ZrS_2) both shifted by 2.0 eV to higher binding energies on the electrochemically cycled crystals. These observations are consistent with an oxide layer formation, which could cause the pH-dependent V_{FB}. Such shifts in V_{FB} for oxides are well documented in the literature (27). The XPS data also suggest that for ZrS_2 simply immersed in the dark in aqueous solution, sulfur atoms on the surface are replaced by oxygen; we observed no peaks for any other sulfur species on the surface, *i.e.*, elemental sulfur, S_x^{-2}, or SO_x. Note that oxide layer formation probably occurs upon immersion of ZrS_2 in the solutions, since the capacitance measurements were made over a potential range where there was very little dark anodic current. Illumination of the electrode with the potential held in the depletion region for several minutes does result in a visible layer of sulfur on the surface, as previously reported (21).

PEC in $Fe^{3+/2+}$ solutions.—The M-S plots for an n-ZrS_2 electrode in 0.10*M* each ferric and ferrous chloride in 1.0*M* HCl at five different frequencies are shown in Fig. 4. Again frequency dependence of *C* is observed with the lines converging on the X-axis. The estimated V_{FB}, −0.23 *vs.* SCE, is close to that for 1*M* HCl in the absence of the $Fe^{3+/2+}$ system. The *i-V* curve for this system under 100 mW/cm² chopped white light illumination is shown in Fig. 3. The onset of anodic photocurrent occurs more than 400 mV negative of the redox potential of the $Fe^{3+/2+}$ system (V_{redox}). The current density (c.d.) at V_{redox} is *ca.* 15 mA/cm². The potential for photocurrent onset is more positive than V_{FB} by about 0.2V. The slow rise of the photocurrent to the saturation probably can be attributed to high recombination rates or slow heterogeneous kinetics. As will be shown later, the doping level of this material is high (*ca.* 1×10^{19} cm^{-3}). This would lead to a relatively narrow space charge region and significant recombination of carriers generated in the low electric field zones of the semiconductor.

A two-electrode cell with a 0.02 cm² area n-ZrS_2 anode and a large Pt gauze cathode, both immersed in 0.1*M* $FeCl_2$, 0.1*M* $FeCl_3$, and 1*M* HCl, was constructed. The photocurrent-voltage curve for this cell, at 2 mV/s scan rate, under 100 mW/cm² white light illumination is shown in Fig. 5. The cell gave a short-circuit photocur-

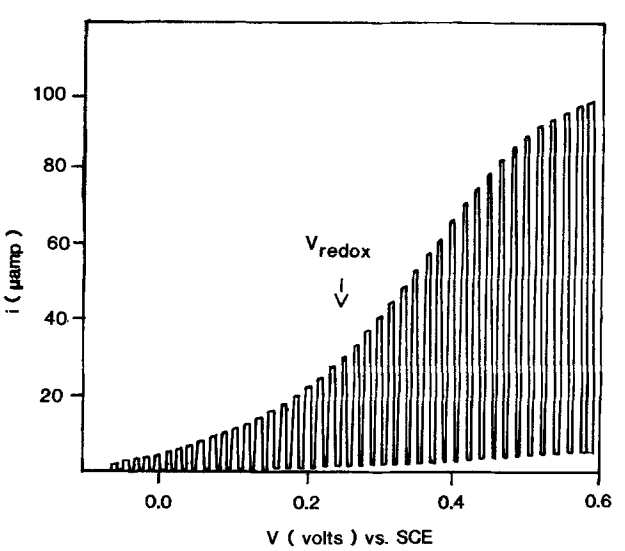

Fig. 7. *i-V* curve for n-ZrS_2 electrode in 0.1M each $K_3Fe(CN)_6$ and $K_4Fe(CN)_6$ (pH = 7.0) under 100 mW/cm², chopped white light illumination. Scan rate: 20 mV/s.

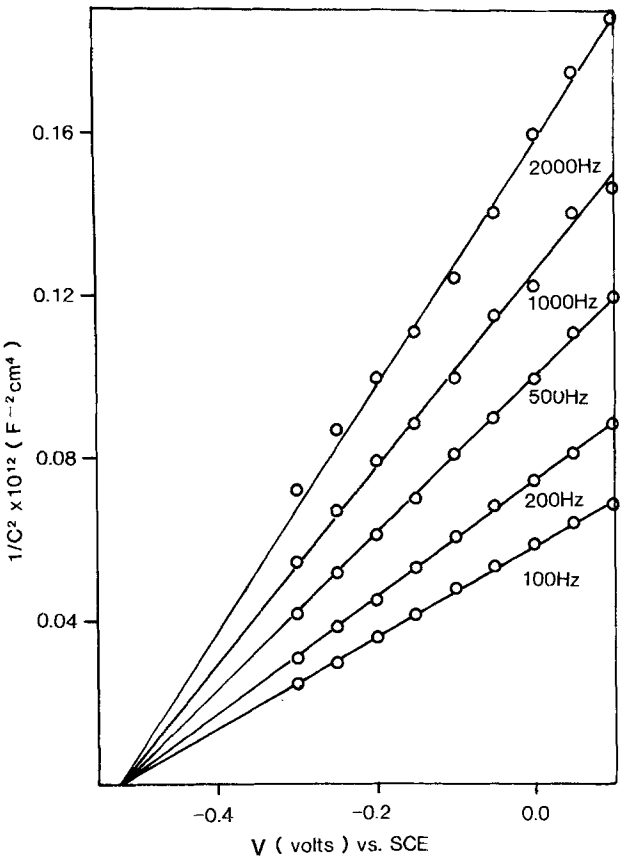

Fig. 8. Mott-Schottky plots for n-ZrS_2 electrode in 1.0M KI (pH = 3.5) at the frequencies indicated.

rent of 0.33 mA and an open-circuit photovoltage of 0.4V. The fill factor was about 0.25. As seen from the *i-V* curves of Fig. 3, the open-circuit photovoltage was lower than that predicted from V_{FB} (−0.23V *vs.* SCE) and V_{redox} (0.46V *vs.* SCE). This probably can be attributed to the cathodic dark reaction at potentials negative of −0.05V and perhaps slow hole transfer from n-ZrS_2 to Fe^{2+}.

$Fe(CN)_6^{3-/4-}$ solution.—The M-S plots for n-ZrS_2 electrode in a solution of 0.10*M* each $K_4Fe(CN)_6$ and $K_3Fe(CN)_6$ at *p*H = 7.0 for five different frequencies in the range 100-2000 Hz are shown in Fig. 6. The V_{FB} is found to be −0.75V. Note that the V_{FB} in the presence of the redox couple is again very near the value predicted in its absence (Fig. 2). The *i-V* curve under 100 mW/cm² white light, chopped illumination is shown in Fig. 7. The onset of photocurrent occurs about 0.3V more negative than V_{redox} (+0.24V *vs.* SCE) at much less negative potentials

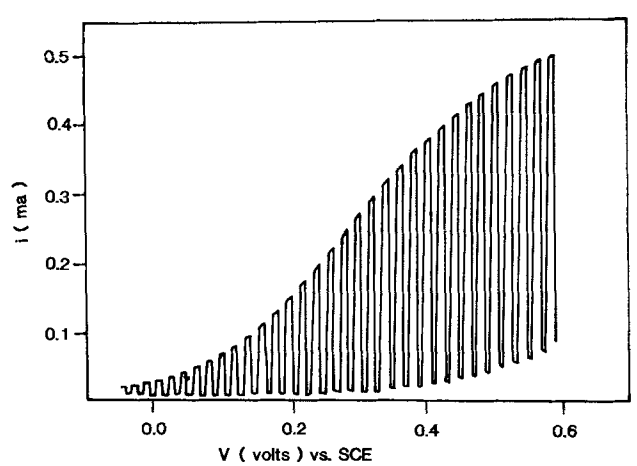

Fig. 9. *i-V* curve for n-ZrS_2 electrode in 1.0M KI (*p*H = 3.5) under 100 mW/cm², chopped white light illumination. Scan rate: 20 mV/s.

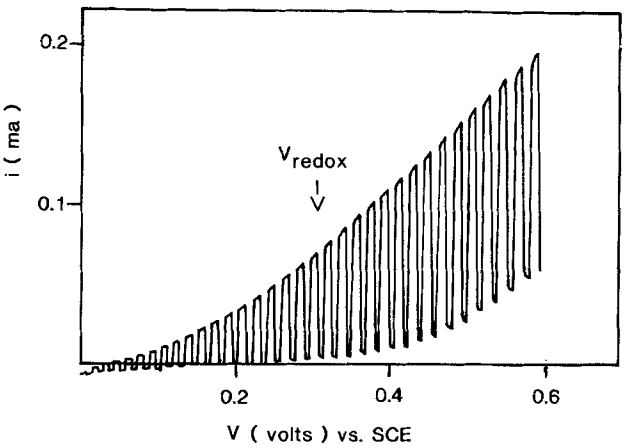

Fig. 10. *i-V* curve for n-ZrS_2 electrode in 1.0M KI and 10 mM I_2 (*p*H = 3.5) under 100 mW/cm², chopped white light illumination. Scan rate: 20 mV/s.

than V_{FB}, and only slowly rises to saturation (beyond V_{redox}), again probably because of slow hole transfer kinetics or large recombination rates. A photocurrent density of 1.3 mA/cm² at V_{redox} is observed.

Iodide solutions.—The M-S plots for n-ZrS_2 in 1.0*M* KI solutions at *p*H 3.5 for five different frequencies are shown in Fig. 8. The V_{FB}, −0.52V *vs.* SCE, is again near the value in iodide-free solutions at this *p*H. Addition of 10 m*M* I_2 to the 1.0*M* KI solution also did not cause a shift in V_{FB}. This lack of effect of I^- and I_3^- on n-ZrS_2, in contrast to other layered materials (3) was also found by Tributsch (21) from photocurrent onset measurements. This lack of I^-/I_2 effect can perhaps be attributed to oxide layer formation that occurs on ZrS_2 in aqueous solutions. The shift in V_{FB} for other layered materials in the presence of I_3^- requires specific adsorption on the surface (3). This adsorption might be decreased by the oxide layer. The *i-V* curve for a 1.0*M* KI solution is shown in Fig. 9. The photocurrent onset is approximately 0.35V

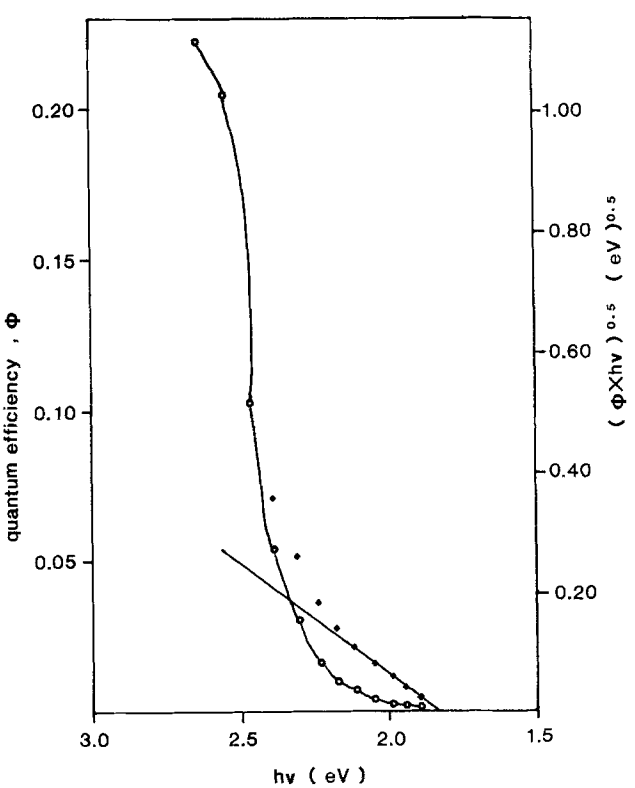

Fig. 11. (a) Photocurrent action spectrum plotted as quantum efficiency (ϕ) *vs.* photon energy ($h\nu$) for n-ZrS_2 in 0.1M each $K_3Fe(CN)_6$ and $K_4Fe(CN)_6$ corrected for solution absorbance (open circles) and (b) $(\phi h\nu)^{1/2}$ *vs.* $h\nu$ for determination of the bandgap, E_g (diamonds).

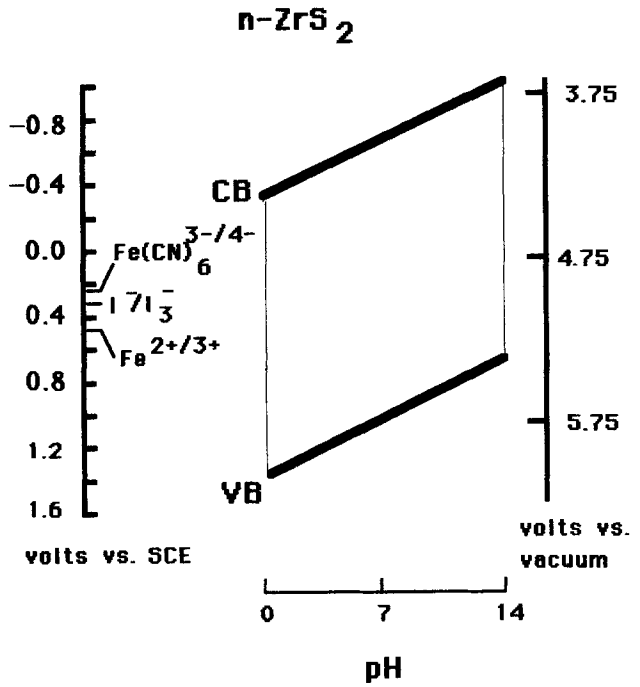

Fig. 12. Band scheme for ZrS_2

negative of the solution redox potential with a photocurrent density of 14 mA/cm² at that potential. Addition of 10 m*M* I_2 to this solution causes the photocurrent density to drop to 3 mA/cm². Moreover, a cathodic current appeared in the *i-V* curve (Fig. 10). This is caused by the reduction of iodine at the electrode surface and is seen with this system in the dark. The decrease in photocurrent in the presence of I_2 is probably mainly attributable to the absorption light by the colored solution, with some I_2 reduction occurring at the less positive potentials. Note also that the shape of the *i-V* curve for the I^-/I_2 system is similar to those of $Fe^{2+/3+}$ and $Fe(CN)_6^{3-/4-}$.

Action spectrum and energy levels.—Knowledge of V_{FB} and E_g allows calculation of an energy level diagram showing the location of the conduction and valence bands. This information is useful in the determination of redox couples for photoelectrochemical (PEC) cells. The action spectrum for n-ZrS_2 in $Fe(CN)_6^{3-/4-}$ is given in Fig. 11a and a plot of $(\phi h\nu)^{1/2}$ *vs.* $h\nu$, where ϕ is the quantum efficiency and $h\nu$ is the photon energy, is given in Fig. 11b. From these plots a value for the indirect gap energy, E_g, of 1.82 ± 0.05 eV for ZrS_2 is obtained. This value agrees well with that reported previously by other types of measurements (16, 17, 28), but is slightly larger than the previous estimate (1.68 eV) from photocurrent measurements (21). A short-circuit quantum efficiency of >20% at 2.6 eV was obtained (without correcting for reflective losses from the mirrorlike surfaces of the crystals).

The M-S data yield $V_{FB} = -0.75$V *vs.* SCE at pH = 7.0. A donor density of 1×10^{19} cm^{-3} was estimated from the slope of the M-S plots in $Fe(CN)_6^{3-/4-}$ where there is little frequency dispersion. A value of 2.5×10^{19} cm^{-3} for the effective density of states in the conduction band can be calculated by taking the effective mass of the electrons, m_e^*, to be *ca.* m_e, the mass of the electron. With these values, ΔE_f, the calculated difference in energy between the conduction band and the Fermi level is very small, *ca.* 0.02 eV. From this the band scheme is derived (Fig. 12) with E_c, the conduction bandedge, at −0.77V *vs.* SCE and the E_v, valence bandedge, at 1.05V *vs.* SCE at pH = 7.0.

Conclusions

Large single crystals of n-ZrS_2 can be prepared by vapor halogen transport techniques. This material shows low dark currents and reasonable photocurrents in ferrous/ferric, ferrocyanide/ferricyanide, and KI solutions, although suffering from slow rise of the photocurrent to saturation (*i.e.*, a poor fill factor) and an open-circuit photopotential that is smaller than that predicted from V_{FB} and V_{redox}. V_{FB} shifts by *ca.* 54 mV for a unit pH change and was unaffected by I_3^-.

Acknowledgment

We thank Professor T. Mallouk for his help and use of his x-ray facilities and Dr. K. A. Pearlstine in obtaining the XPS data. N. C. thanks ICSU/UNESCO for the award of Distinguished Fellowship in Science and to Director of CECRI for the grant of one year leave. The support of this research by the National Science Foundation (CHE8304666) is gratefully acknowledged. The XPS instrumentation used in this research was supported in part by the National Science Foundation (CHE8201179).

Manuscript submitted Jan. 1, 1986; revised manuscript received June 6, 1986.

The University of Texas at Austin assisted in meeting the publication costs of this article.

REFERENCES

1. H. Tributsch, *Ber. Bunsenges. Phys. Chem.*, **81,** 361 (1977).
2. H. D. Abruna, G. A. Hope, and A. J. Bard, *This Journal,* **129,** 2224 (1982).
3. F.-R. F. Fan and A. J. Bard, *ibid.*, **128,** 945 (1981).
4. J. Gobrecht, H. Tributsch, and H. Gerischer, *ibid.*, **125,** 2085 (1978).
5. S. Prybyla, W. S. Struve, and B. A. Parkinson, *ibid.*, **131,** 1587 (1984).
6. K. Rajeshwar, *J. Appl. Electrochem.*, **15,** 1 (1985).
7. J. V. Marzik, R. Kershaw, K. Dwight, and A. Wold, *J. Solid State Chem.*, **51,** 170 (1984).
8. B. L. Wheeler, J. K. Leland, and A. J. Bard, *This Journal,* **133,** 358 (1986).
9. H. Tributsch, *Ber. Bunsenges. Phys. Chem.*, **82,** 169 (1978).
10. K. Kalyanasundaram, *Solar Cells,* **15,** 93 (1985).
11. J. Gobrecht, H. Gerischer, and H. Tributsch, *Ber. Bunsenges. Phys. Chem.*, **82,** 1331 (1978).
12. W. Kautek and H. Gerischer, *ibid.*, **84,** 645 (1980).
13. H. Tributsch, *Struct. Bonding,* **49,** 127 (1982).
14. L. F. Schneemeyer and M. S. Wrighton, *J. Am. Chem. Soc.*, **101,** 6496 (1979).
15. J. A. Wilson and A. D. Yoffe, *Adv. Phys.*, **18,** 193 (1969).
16. A. R. Beal, J. C. Knight, and W. Y. Liang, *J. Phys. C,* **5,** 3531 (1972).
17. H. P. Hughes and W. Y. Liang, *ibid.*, **10,** 1078 (1977).
18. H. S. White, F.-R. F. Fan, and A. J. Bard, *This Journal,* **128,** 1045 (1981).
19. G. Nagasubramanian, B. L. Wheeler, and A. J. Bard, *ibid.*, **130,** 1680 (1983).
20. G. Nagasubramanian, B. L. Wheeler, G. A. Hope, and A. J. Bard, *ibid.*, 130, 385 (1983).
21. H. Tributsch, *ibid.*, **128,** 1261 (1981).
22. H. Schaffer, "Chemical Transport Reactions," Academic Press, Inc., New York (1964).
23. R. Kershaw, M. Vlasse, and A. Wold, *Inorg. Chem.*, **6,** 1599 (1967).
24. C. N. R. Rao and K. P. R. Pisharody, *Prog. Solid State Chem.*, **10,** 207 (1979).
25. E. C. Dutoit, R. L. Van Meirhaeghe, F. Cardon, and W. P. Gomes, *Ber. Bunsenges. Phys. Chem.*, **79,** 1206 (1975).
26. H. Tributsch and J. C. Bennett, *J. Electroanal. Chem. Interfacial Electrochem.*, **81,** 97 (1977).
27. For example, see: (a) M. A. Butler and D. S. Ginley, *This Journal,* **125,** 228 (1978); (b) D. E. Scaife, *Sol. Energy,* **25,** 41 (1980); (c) P. J. Boddy and W. H. Brattain, *This Journal,* **110,** 570 (1963).
28. D. L. Greenaway and R. Nitsche, *J. Phys. Chem. Solids,* **26,** 1445 (1965).